THE ASTROPHYSICAL JOURNAL, 563:L161–L164, 2001 December 20

THE NARROWBAND ULTRAVIOLET IMAGING EXPERIMENT FOR WIDE-FIELD SURVEYS. I. DUST-SCATTERED CONTINUUM

D. SCHIMINOVICH,[1,2] P. G. FRIEDMAN,[1,2] C. MARTIN,[1,2] AND P. F. MORRISSEY[2]
Received 2001 October 1; accepted 2001 November 13; published 2001 December 4

ABSTRACT

We report on the first results of NUVIEWS, a sounding rocket experiment designed to map the far-UV background in four narrow UV bands. This is the first imaging measurement of the UV background to cover a substantial fraction of the sky. In our first flight, we mapped one-quarter of the sky with ~5′–10′ imaging resolution. We present a map of the continuum background obtained in the 1740 Å telescope and use a model based upon the multiple scattering approach of Witt, Friedman, & Sasseen and a three-dimensional stellar distribution to constrain the dust and other parameters. We find that the dust in the diffuse interstellar medium displays a moderate albedo ($a = 0.45 \pm 0.05$) and highly forward scattering phase function parameter ($g = 0.77 \pm 0.1$) over a large fraction of the sky, similar to the result found for a more restricted area by Witt, Friedman, & Sasseen. We have also discovered a significant variance from the model and shown that it is a natural property of the statistics of clouds with varying multiple scattering geometries. The coverage and quality of our data allows us to place simultaneous constraints on a, g, the extragalactic background (200 ± 100 CU), a slant cosecant (airglow) contribution (~200 CU), and an instrumental scattering component (40 ± 30 CU).

Subject headings: radiative transfer — scattering — ultraviolet: ISM

1. INTRODUCTION

Paresce & Jakobsen (1980) presented the first evidence for a correlation between the far-ultraviolet (FUV) continuum background and Galactic H I, thereby determining that most of the background is Galactic in origin, consistent with scattering of the integrated UV radiation field by pervasive interstellar dust associated with gas clouds. This correlation is typically expressed as a slope of FUV continuum intensity versus neutral hydrogen column $N_{\rm H\,I}$ and has been measured by many different investigators, as summarized in Bowyer [1991; $I_{\rm FUV} \simeq (0.3\text{–}2.5)N_{\rm H\,I} + 300$].[3] The wide variation in measured slope is very likely due to variations in the dust properties and anisotropies of the illuminating UV stellar radiation field.

Dust properties extracted from such studies are the albedo a and the asymmetry parameter of the Henyey-Greenstein scattering phase function g. Witt, Friedman, & Sasseen (1997, hereafter WFS) used a Monte Carlo model of the cloud structure of the interstellar medium (ISM) and FUV stellar fluxes from the TD-1 catalog (Gondhalekar, Philips, & Wilson 1980) to create a two-dimensional radiation field. They compare the model to measured diffuse background fluxes in 14 fields obtained with the FAUST experiment (Bowyer et al. 1993). They determine an albedo of 0.45 ± 0.05 with an asymmetry factor of $g = 0.68 \pm 0.10$. The dust albedo is 50% lower than that seen in reflection nebulae, suggesting a difference between grain sizes (e.g., H II regions show a deficiency of small grains; Baldwin et al. 1991).

WFS use their model to show that *the nonisotropic phase function and radiation field produce a wide range of* $I_{\rm FUV}/N_{\rm H\,I}$ *slopes and could account for the wide variation in measured values.* The FAUST measurements produced a high $I_{\rm FUV}/N_{\rm H\,I}$ slope (~2.5) CU $(10^{18}\ {\rm cm}^{-2})^{-1}$ because forward-scattering grains couple the bright stars in the plane below to the diffuse radiation field. Correspondingly, an isotropic model would underpredict the albedo in a quadrant deficient of stars, as was the case for the UV experiment mission (Hurwitz, Bowyer, & Martin 1991).

We present in this Letter the first results from an experiment specifically designed to spectrally isolate and globally map the components of the cosmic UV background. We focus here on the dust-scattered continuum and the implications for the properties of the dust in the diffuse ISM.

2. INSTRUMENT/FLIGHT

The Narrowband Ultraviolet Imaging Experiment for Wide-Field Surveys (NUVIEWS) is a rocket-borne instrument that maps line and continuum components of the FUV background across one-quarter of the sky (~10,000 deg^2) in 300 s during a single flight. The experiment contains four co-aligned, wide-field (20° × 30°), self-filtering telescopes with imaging, photon-counting, microchannel plate detectors. The four telescopes have bands centered on C IV (1550 Å), the peak of the H_2 Lyman fluorescence band (1610 Å), and two relatively line 'free regions (1450 and 1740 Å) with bandwidths of 70–100 Å. The experiment was carefully designed to significantly attenuate the contributions from off-band airglow lines, geocoronal Lyα, earthshine, and moonlight. All instrument surfaces and baffles provide the maximum possible stray and scattered light rejection, given the constraints of a wide-field mission.

This Letter concentrates exclusively on data from the fourth band (1740 Å, 100 Å FWHM, 1.46 cm^2 Å effective area–bandwidth product), which is a region relatively free of molecular and atomic transition lines, ideal for studying dust-scattered FUV continuum light. A fused silica filter placed in front of the detector (cutoff 1590 Å) reduced the signal from the strong geocoronal Lyα and O I (1304 and 1356 Å) airglow lines. The instrumental angular resolution in this band was 5′–10′ FWHM.

The payload was launched at 07:15:00.7 UT on 1996 July 14. NUVIEWS implemented a zigzag pattern consisting of eight scans of 90° in length (measured using the field center) with the whole rectangular scan area centered on $19^{\rm h}$, +30°. All data presented in this Letter were acquired during the 287 s that the payload was above an altitude of 150 km. The average exposure

[1] Department of Physics, Columbia University, 538 West 120th Street, New York, NY 10027.
[2] Present address: Division of Physics, Mathematics, and Astronomy, California Institute of Technology, MS 405-47, Pasadena, CA 91125.
[3] $N_{\rm H\,I}$ in units of 10^{18} H I cm^{-2}; $I_{\rm FUV}$ in continuum units (CU); 1 CU = 1 photon cm^{-2} sr^{-1} s^{-1} Å^{-1}.

over the whole scan area was 15 s. Detector background was low (<1 counts cm^{-2} s^{-1}), corresponding to less than 25% of the lowest anticipated diffuse Galactic background signal.

3. CALIBRATION AND DATA ANALYSIS

The TD-1 database of FUV (1565 and 1975 Å) stellar photometry (Gondhalekar et al. 1980) is the ideal catalog for comparison with our images, since the TD-1 3 σ detection limit (1×10^{-12} ergs cm^{-2} $Å^{-1}$ s^{-1}) is just below our 3 σ detection limit (4×10^{-12} ergs cm^{-2} $Å^{-1}$ s^{-1}), and we can determine the position and cross calibrate a flux for nearly every star that we detect. A small fraction of stars that we detected were not in the TD-1 catalog (<2%). The TD-1 absolute flux scale is accurate to 10% and nonlinear only below fluxes of 1.0×10^{-12} ergs cm^{-2} $Å^{-1}$ s^{-1} (Bowyer et al. 1993). Our flight data calibration used stars within a flux range of (1–100) $\times 10^{-11}$ ergs cm^{-2} $Å^{-1}$ s^{-1} for cross calibration with the TD-1 catalog to avoid TD-1 nonlinearities and bright stars that saturated on our detectors.

After applying corrections for telescope plate scale, distortions and offsets, detector spatial nonlinearities, position offsets, pulse-height dependencies, rotations, and thermal drift, we used detected stars and their TD-1 positions to aspect-correct our photon data. This resulted in images with 8′–10′ FWHM star profiles. Star-subtracted sky flat-field images were generated in detector coordinates using the complete set of scan data. Normalized, distortion-corrected sky flat fields were combined with the aspect solution to generate exposure sky maps corresponding to the instrument area–bandwidth exposure product. The absolute calibration of these maps was refined based on in-flight measurements of TD-1 stars.

We then generated exposure-corrected, detector background subtracted, 20° × 20° field maps on 15° centers. When studying the background, extended point-spread function (PSF) halos can produce a spurious signal, particularly in regions around bright stars. The calibrated PSF was compared with the in-flight data using stars with no apparent dust halo, to 5° radius. Simulated maps of the TD-1 fields convolved with the telescope PSF were generated for each field and subtracted from the calibrated data maps. This allowed us to accurately subtract the flux due to the stellar component as well as to refine the instrument flux calibration, which agreed within systematic and random errors with postcalibration throughput measurements.

Since some detected stars are not present in the TD-1 catalog and the subtraction at the peak of the PSF is not perfect, we blanked (~1° diameter) around TD-1 star locations and other peak detections. The remaining unmasked flux was binned into square bins of 3.°75, 5°, and 6.°25 on a side. Heavily masked bins, or bins with low exposure (e.g., at the edge of the scan pattern), were flagged and omitted from the subsequent analysis. The 6.°25 binned data, in 250 independent bins or "pixels," were used for comparison with our dust-scattering model, described in § 4. We obtained values for $N_{\rm H\,I}$ and $I_{\rm IR}$ for each bin, using only data from the unmasked regions in our field maps. (Composite H I maps from Dickey & Lockman 1995 and 100 μm IR maps from Schlegel, Finkbeiner, & Davis 1998.) We plot $I_{\rm FUV}$ versus $N_{\rm H\,I}$ in Figure 1, where a significant correlation is apparent.

We also constructed a dust-scattered continuum sky map, shown in Figure 2. In generating this image, we smoothly interpolated over masked regions using a ~1.°5 smoothing diameter. The sky map reveals dust-scattered halos around bright stars (e.g., near the Upper Scorpius reflection nebula at $l = 0°$, $b = 20°$) and a strong gradient decreasing upward from the plane. Also evident is a clear variation with Galactic longitude. There exists a significant depression in dust-scattered continuum light at high latitudes above less intense segments of the Galactic plane from $l = 20°$ to $l = 60°$.

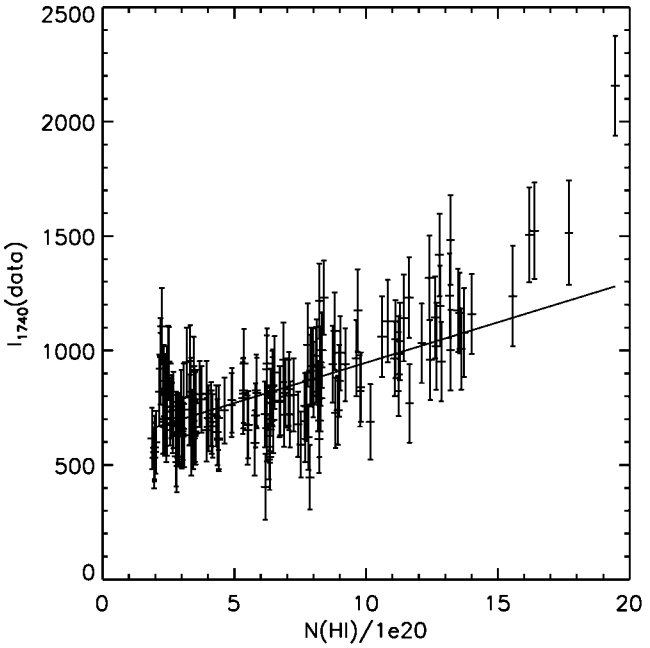

FIG. 1.—Intensity in the 1740 Å map (in CU) vs. $N_{\rm H\,I}$ column density (in units of 10^{20} cm^{-2}), for $b_{\rm min} = 22.°5$. Error bars include cosmic variance component (see text). Best fit is line with slope 0.42 CU $(10^{18}\ cm^{-2})^{-1}$, offset 530 CU.

4. DUST-SCATTERING MODEL

We have developed a dust-scattering radiative transfer model to fit the continuum data. The model incorporates elements of the WFS model, including multiple scattering in clouds. However, the model includes two important refinements. First, rather than using a two-dimensional radiation field with corrections for the illumination of clouds off the Galactic plane, we use a true three-dimensional field. The radiation field is generated by placing TD-1 UV catalog stars at three-dimensional locations in space given by the *Hipparcos* reference catalog (European Space Agency 1997) distances. Stars producing 98% of the UV radiation field have *Hipparcos* parallaxes. For computational efficiency, we produce from this a grid of complete two-dimensional radiation fields at various locations in three-dimensional space where clouds might appear along the line of sight (five dimensions total). The radiation field at each location is calculated by modifying the flux vector for each star for the new location and optical depth. The latter is calculated assuming dust is distributed in a homogenous exponential layer with a scale height of 110 pc. A second refinement is that we also calculate the diffuse galactic light for each albedo and phase function grid point, for a one-dimensional grid of positions above or below the Galactic plane. We modify observed dust column densities (Schlegel et al. 1998) using the same exponential dust model. This calculated diffuse galactic light is added to the stellar radiation field to determine the total cloud illumination.

Following WFS, for each line of sight in our map we calculate (statistically) the distribution of cloud numbers and types that produces this $N_{\rm H\,I}$ and the corresponding scattered intensity. The

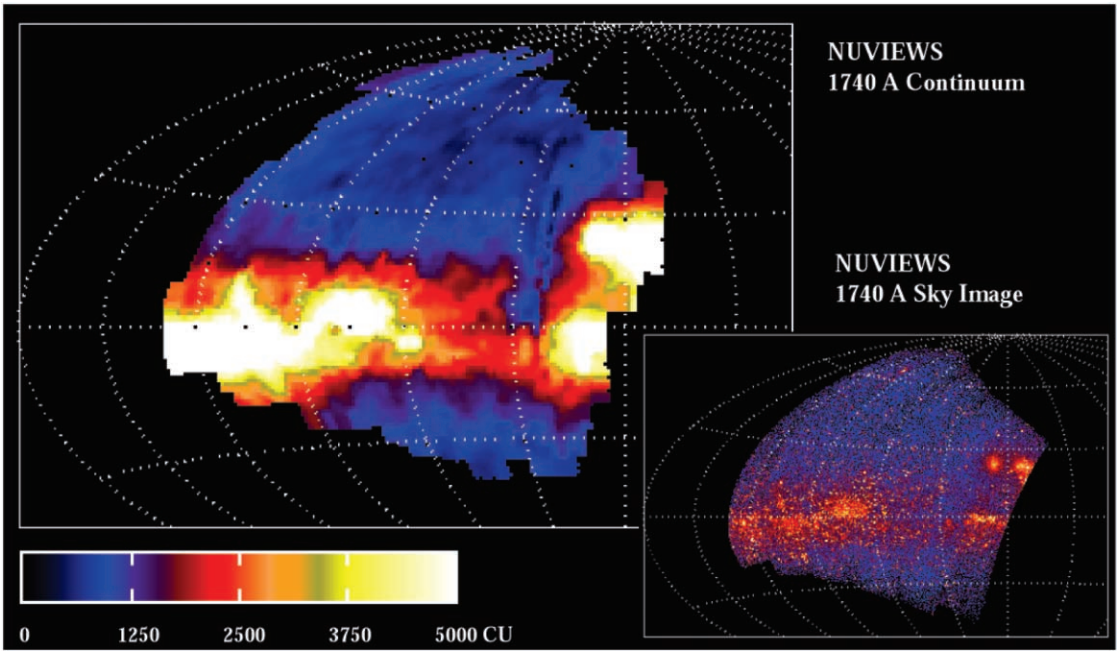

FIG. 2.—NUVIEWS 1740 Å calibrated sky maps using Flight 1 data. Aitoff projections are centered on Galactic center. *Main image:* Star-subtracted continuum map. Color bar indicates intensity in CU. Pixel size is 1° × 1°. *Inset image:* Sky map with stars included. Color is scaled to the cube root of the intensity, in arbitrary units. Pixel size is 0.°5 × 0.°5.

model calculates surface brightnesses for three types of cloud (central optical depth 0.5, 2.5, 10) with line-of-sight frequency of 12 : 3 : 1. These are illuminated by the corresponding radiation field for their location. The resulting surface brightness includes the effects of multiple scattering in the cloud, calculated for a grid of albedos and phase function parameters (a, g). Several hundred realizations are calculated for each line of sight to obtain an average intensity. The model makes a definite prediction for the intensity at every point in the map. When we use our model to fit the FAUST data presented in WFS, we obtain $a = 0.5^{+0.10}_{-0.05}$, $g = 0.80 \pm 0.10$, and $I_0 = 750 \pm 200$ CU (where the latter is the airglow "offset") versus the WFS result of $a = 0.45 \pm 0.05$, $g = 0.68 \pm 0.1$, and $I_0 = 540 \pm 140$. The results differ slightly but are formally in agreement.

When we compare the model with the 1740 Å NUVIEWS data, we perform several data cuts. We use only data with exposure times exceeding 10 s, bins that have more than 20% of their area remaining after star blanking, and no bins at the edges of the map. We excluded two regions with clear stellar dust halos and three anomalously low bins.

Our model also predicts the variance that is to be expected owing to our incomplete knowledge of the precise cloud geometry with respect to the anisotropic radiation field. Clouds that have typical diffuse ISM densities will nearly fill the 6.°25 bin at typical distances. Differences in the cloud geometry, impact parameter, and multiple scattering along the line of sight can produce the same $N_{\rm H\,I}$ but with different total scattered intensity. We can estimate these variance sources using our model for a random ensemble of cloud types, impact parameters, and heights above the Galactic plane that produce the same $N_{\rm H\,I}$. The approximate result is a model variance with $\sigma_I^2 = kI$ and $k \simeq 20$–30 CU. The variance increases linearly with the intensity and the total number of clouds along the line of sight. Thus, our variance model provides a quantitative statistical foundation for evaluating the confidence limits on the model parameters.

A χ^2 comparison of the mean model and data show that a significant additional source of variance is in fact present. We have verified that this variance is not correlated with the brightness of stars that are removed or star halos that are subtracted from the maps. We have proven that the variance is not produced by instrumental scattering. We did this by using the model to generate a series of scattered intensities for fixed column density, impact parameter, and local cloud location for a highly forward scattering phase function. This simulates the effect of instrumental scattering on the observed intensity distribution. The addition of a variable amount of this foreground scattering component produces at best a 5% reduction in variance with at most a modest scattering component ($I \simeq 30$ CU at high b) and no effect on other best-fit parameters. The best fit is statistically consistent with no foreground scattering at 90% confidence. We find no evidence for any other variance introduced by the instrument or analysis. We therefore attribute the observed variance to the "cosmic variance" predicted by the multicloud model.

Even with this "cosmic variance," a χ^2 comparison yields a tight limit on acceptable (a, g) pairs; our model predictions are robust over a wide range of assumptions and data cuts. The model includes as adjustable parameters an extragalactic background light (EBL) or halo background component with appropriate absorption in the galaxy (calculated by the model) and an additional component I_0 that is modeled as either a constant offset or proportional to the slant cosecant through the residual atmosphere. The χ^2 for the slant case is far lower than for the constant case ($\chi^2_{\rm slant} = 194$, $\chi^2_{\rm const} = 277$, both for 171 degrees of freedom), strongly suggesting that the residual offset is due to airglow emission.

We also tested for the impact of unresolved, unmasked stars on the results using the *Hipparcos* catalog to estimate UV fluxes in each bin based on the distance, $N_{\rm H\,I}$, stellar type, and V magnitude. Assuming very conservatively that all stars with a flux of 10^{-11} ergs cm^{-2} s^{-1} Å^{-1} (10 times higher than the

TABLE 1
CONTINUUM MODEL FIT SUMMARY

								$c_{\rm H\,I}$ [b]		c_d [c]	
$b_{\rm min}$	SLANT	a	g	χ^2 [a]	dof	$I_{\rm EBL}$	I_0	Model	Data	Model	Data
15.0	Yes	0.46 ± 0.05	0.79 ± 0.05	320	236	100 ± 100	230 ± 30	0.46	0.51	1.07	1.12
22.5	Yes	0.45 ± 0.05	0.77 ± 0.07	194	171	200 ± 100	190 ± 40	0.35	0.48	0.78	0.81
22.5	No	0.5 ± 0.1	0.77 ± 0.07	276	171	500^{+0}_{-300}	0^{+200}_{-0}	0.43	0.48	0.81	0.81
30.0	Yes	0.40 ± 0.15	0.75 ± 0.08	159	143	100^{+250}_{-100}	240^{+40}_{-100}	0.37	0.27	0.60	0.58

[a] Includes cosmic variance with $\sigma_I^2 = 25I$ (CU).
[b] Units CU $(10^{18}\ {\rm cm}^{-2})^{-1}$ (H I from Dickey & Lockman 1995).
[c] Units CU $(0.01\ {\rm MJy\ sr}^{-1})^{-1}$ (100 μm IR from Schlegel et al. 1998).

TD-1 catalog cutoff) are unaccounted for and add to the diffuse maps, we find that the median effective intensity contribution is 21 CU, with 40 CU as a mean. Adding these stars to the model in the appropriate map bins, we find that the inferred dust parameters and offset are essentially unchanged.

We performed several Galactic latitude cuts in order to restrict our analysis to uncrowded regions above the Galactic plane. With a minimum latitude cut of 22°.5, we find $a = 0.45 \pm 0.05$, $g = 0.77 \pm 0.07$, $f_{\rm scat} = 1.00 \pm 0.75$ ($f_{\rm scat} = 1$ corresponds to $I_{\rm scat} \simeq 30$ CU at $b = 90°$) $I_{\rm EBL} = 200 \pm 100$ CU, and the airglow contribution $I_0 = 190 \pm 40$ CU at zenith. This reduced data set covers 6500 deg^2 on the sky. Values obtained with different latitude cuts all produce overlapping 90% confidence intervals, all consistent with the above limits. We also calculated the slope of the data versus $N_{\rm H\,I}$, IRAS 100 μm, and csc b, compared with the various models. The best-fit models reproduce all three slopes reasonably well. A summary is presented in Table 1, and the data and best-fit model are compared in Figure 3.

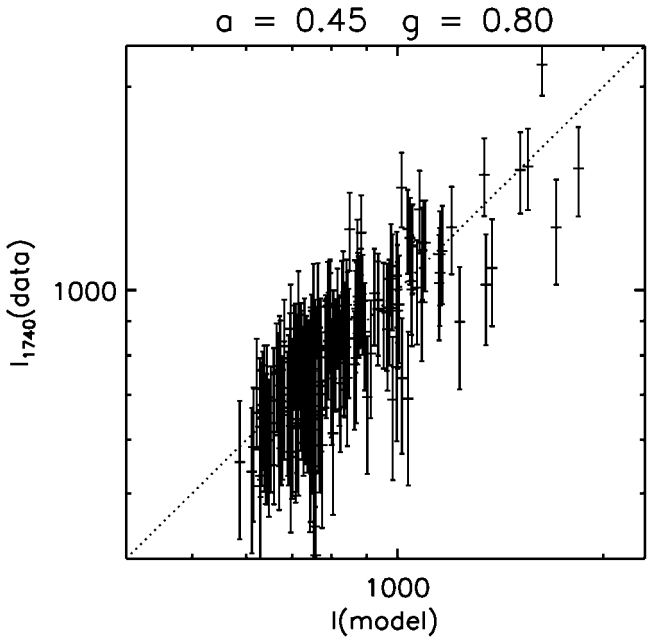

FIG. 3.—Intensity in the 1740 Å map (in CU) vs. model 2a, for $b_{\rm min} = 22°.5$. Error bars include cosmic variance component (see text).

5. SUMMARY

The NUVIEWS survey is unique in combining significant sky coverage over a contiguous region, with good imaging and star removal. It provides the first global measure of the properties of the dust-scattered continuum while also measuring local variations with significance.

Our measured slope (0.35–0.50) is among the lowest slopes yet measured but is consistent with the weaker stellar radiation field observed at these longitudes. We thus confirm the prediction of WFS that the slope can vary by a factor of more than 5 owing to the anisotropic radiation field. The best model fit values for albedo and phase function asymmetry ($a = 0.45 \pm 0.1$, $g = 0.77 \pm 0.1$) are comparable to the values measured from the diffuse radiation field by WFS and somewhat lower than the albedos found for dust scattering in star-forming regions (Calzetti et al. 1995; Witt et al. 1992). We thus confirm the dust properties found by WFS over a much larger fraction of the sky. We can also independently constrain the extragalactic background, which appears to be in the range of 200 ± 100 CU.

We have identified both the source of the offset (a slant cosecant term, probably airglow) and cosmic variance (cloud variation combined with multiple scattering, and three-dimensional radiation field variance) and placed new constraints on the extragalactic background. We anticipate that completion of the NUVIEWS all-sky survey should confirm and strengthen these conclusions.

We gratefully acknowledge Steven Kaye, Irwin Rochwarger, Judy Fleischman, Peter Marshall, and Muamer Zukic and NASA project manager David Kotsifakis and his team for work on the sounding rocket payload. This work was supported by NASA grants NAG 5-642 and NAG 5-5052 and by funding from the California Institute of Technology.

REFERENCES

Baldwin, J. A., Ferland, G. J., Martin, P. G., Corbin, M. R., Cota, S. A., Peterson, B. M., & Slettebak, A. 1991, ApJ, 374, 580
Bowyer, S. 1991, ARA&A, 29, 59
Bowyer, S., Sasseen, T., Lampton, M., & Wu, X. 1993, ApJ, 415, 875
Calzetti, D., Bohlin, R. C., Gordon, K. D., Witt, A. N., & Bianchi, L. 1995, ApJ, 446, L97
European Space Agency. 1997, The *Hipparcos* and Tycho Catalogs, ed. M. A. C. Perryman (ESA SP-1200; Noordwijk: ESA)
Dickey, J. J., & Lockman, F. J. 1995, Astron. Data Image Library, L1
Gondhalekar, P. M., Phillips, A. P., & Wilson, R. 1980, A&A, 85, 272
Hurwitz, M., Bowyer, S., & Martin, C. 1991, ApJ, 372, 167
Paresce, F., & Jakobsen, P. 1980, Nature, 288, 119
Schlegel, D. J., Finkbeiner, D. P., & Davis, M. 1998, ApJ, 500, 525
Witt, A. N., Friedmann, B. C., & Sasseen, T. P. 1997, ApJ, 481, 809 (WFS)
Witt, A. N., Petersohn, J. K., Bohlin, R. C., O'Connell, R. W., Roberts, M. S., Smith, A. M., & Stecher, T. P. 1992, ApJ, 395, L5